Measurement of the Wigner Distribution and the Density Matrix of a Light Mode Using Optical Homodyne Tomography: Application to Squeezed States and the Vacuum

D. T. Smithey, M. Beck, and M. G. Raymer

Department of Physics and Chemical Physics Institute, University of Oregon, Eugene, Oregon 97403

A. Faridani

Department of Mathematics, Oregon State University, Corvallis, Oregon 97331

We have measured probability distributions of quadrature-field amplitude for both vacuum and quadrature-squeezed states of a mode of the electromagnetic field. From these measurements we demonstrate the technique of optical homodyne tomography to determine the Wigner distribution and the density matrix of the mode. This provides a complete quantum mechanical characterization of the measured mode.

According to the standard interpretation of quantum mechanics the density matrix $\hat{\rho}$ contains all knowable information about a given quantum system and allows the most precise statistical predictions possible. A measurement of the density matrix would provide a complete characterization of novel quantum states, including squeezed states [1,2] and states yet to be produced such as macroscopic superpositions (Schrödinger cat states). In general, a set of probability distributions measured in different representations is sufficient to determine $\hat{\rho}$ uniquely [3]. For a system with a single degree of freedom, described by an operator $\hat{x}$, one can define quadrature amplitudes $\hat{x}_\phi$ which are related to $\hat{x}$ by Hilbert-space rotations. Vogel and Risken [3] recently showed that one can obtain the Wigner distribution by tomographic inversion of a set of measured probability distributions, $P_\phi(x_\phi)$, of the quadrature amplitudes. Since there is a one-to-one correspondence between the Wigner function and the density matrix [4], their proposed method accomplishes the measurement of $\hat{\rho}$. Alternative measurement methods for determining the state of a system have been suggested by Royer [5] and by Band and Park [6]. To date, no reports have been made of quantum state measurements on systems with continuous variables.

In this paper we report the first measurements of quadrature-amplitude distributions for a mode of the electromagnetic field obtained using balanced homodyne detection. From the measured distributions, we determine the Wigner distribution and density matrix in the cases of vacuum and quadrature-squeezed states. Our measurements are in contrast to previous experiments involving homodyne detection, which measured the quadrature variances. In general, measurements of variances are not sufficient to fully characterize the quantum state. It is essential to measure $P_\phi(x_\phi)$ if one wishes to extract the density matrix for an arbitrary state. Once the distributions $P_\phi(x_\phi)$ are obtained, we use the inverse Radon transform familiar in tomographic imaging to obtain the

Wigner distribution and density matrix. We refer to this new method as optical homodyne tomography (OHT). The application of OHT to a squeezed state agrees well with the theoretical predictions. We point out that the method of OHT applies to any state without assuming a particular form for $P_\phi(x_\phi)$.

The Wigner phase-space distribution for a single degree of freedom is defined as [4]

$$W(x,p) = \frac{1}{\pi} \int_{-\infty}^{\infty} \langle x+x'|\hat{\rho}|x-x'\rangle e^{-2ipx'} dx', \qquad (1)$$

where $\hat{\rho}$ is the density operator and $|x\rangle$ is an eigenstate of the operator $\hat{x}$, obeying $[\hat{x},\hat{p}]=i$ with its conjugate variable $\hat{p}$. In the case of a pure state there is a unique correspondence between the wave function $\psi(x)=\langle x|\psi\rangle$ and the density matrix through the relation $\langle x|\hat{\rho}|x'\rangle = \psi(x)\psi^*(x')$. For a light mode with annihilation operator $\hat{a}$, the operators $\hat{x}$ and $\hat{p}$ are $\hat{x}=(\hat{a}+\hat{a}^\dagger)/2^{1/2}$ and $\hat{p}=(\hat{a}-\hat{a}^\dagger)/i2^{1/2}$. The Wigner distribution is a joint quasiprobability distribution and is especially suited for calculating statistical moments of the quadrature amplitudes represented by the operators

$$\hat{x}_\phi = \hat{x}\cos\phi + \hat{p}\sin\phi, \quad \hat{p}_\phi = -\hat{x}\sin\phi + \hat{p}\cos\phi, \qquad (2)$$

defined with respect to a reference phase ϕ. Any moment involving $\hat{x}$ and $\hat{p}$ in Weyl order can be evaluated as a c-number integral with $W(x,p)$ as a joint weighting function, even though for some states $W(x,p)$ can be negative over portions of its domain [4]. Furthermore, the probability distribution $P_\phi(x_\phi)$ for any quadrature amplitude x_ϕ can be obtained by integrating the Wigner distribution over the conjugate variable p_ϕ [3],

$$P_\phi(x_\phi) = \int_{-\infty}^{\infty} W(x_\phi\cos\phi - p_\phi\sin\phi, x_\phi\sin\phi + p_\phi\cos\phi) dp_\phi. \qquad (3)$$

Given a set of distributions $P_\phi(x_\phi)$ measured by homodyne detection, for all values of ϕ between 0 and π, Eq. (3) can be inverted to yield $W(x,p)$ [3]. For a finite set

of ϕ values, the inversion can be carried out using the inverse Radon transform familiar in tomographic imaging [7]. This is the basis of optical homodyne tomography.

The measured Wigner distributions for a quadrature-squeezed state and for the vacuum state of a field mode are shown in Fig. 1. In our implementation of balanced homodyne detection a pulsed signal field E_S is superposed by a 50/50 beam splitter with a pulsed coherent-state field $E_{\rm LO}$, called the local oscillator (LO), with phase ϕ [8]. The resulting fields are detected with high-quantum-efficiency photodiodes, and the resulting current pulses are temporally integrated and subtracted. This yields the photoelectron difference number N_ϕ. Recently we showed that our apparatus allows the measurement of distributions of photoelectron difference number in the macroscopic domain [9]. The subtraction eliminates classical-like fluctuations of the LO and signal fields, allowing the quantum nature of the signal to be detected [8]. Assuming the LO to be much stronger than the signal, the operator N_ϕ for total photoelectron difference number is proportional to the quadrature-amplitude operator, defined with respect to the LO phase ϕ by [10, 11]

$$\hat{x}_\phi = \hat{N}_\phi / (2\bar{n}_{\rm LO})^{1/2}, \tag{4}$$

where $\bar{n}_{\rm LO}$ is the mean photoelectron number produced by the LO pulse. For homodyne measurement using a photodetector having quantum efficiency η and response time longer than the LO pulse duration, the annihilation operator $\hat{a}$ related to the quadrature amplitude $\hat{x}_\phi$ is given by $\hat{a} = \sqrt{\eta}\hat{a}_s + \sqrt{1-\eta}\hat{a}_{\rm vac}$, where [12]
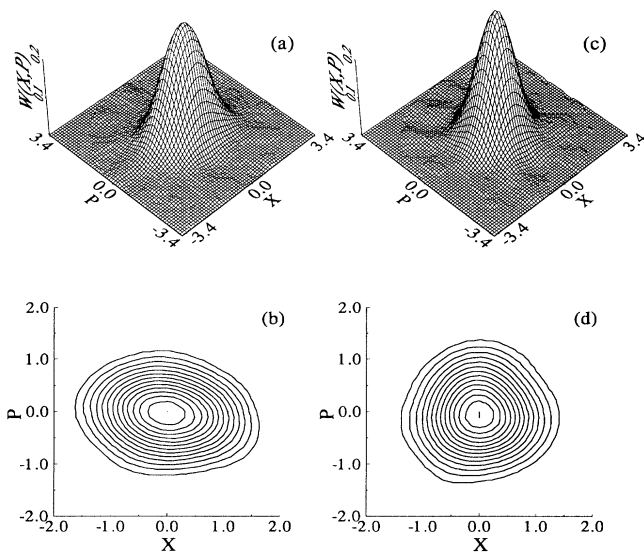

FIG. 1. Measured Wigner distributions for (a),(b) a squeezed state and (c),(d) a vacuum state, viewed in 3D and as contour plots, with equal numbers of constant-height contours. Squeezing of the noise distribution is clearly seen in (b).

$$\hat{a}_s = -i(c/2\pi\hbar\bar{\omega})^{1/2}\int_A d^2s \int_0^T dt\, u_{\rm LO}(\mathbf{s},t)\hat{E}_S^{(+)}(\mathbf{s},t), \tag{5}$$

and $\hat{a}_{\rm vac}$ is a vacuum operator coupled in by the loss mechanism [10]. The interval $[0,T]$ fully contains the pulses and $\hat{E}_S^{(+)}(\mathbf{s},t)$ is the positive-frequency part of the signal-field operator at the detectors' faces. The mode function $u_{\rm LO}(\mathbf{s},t)$ is related to the c-number LO field $E_{\rm LO}^{(-)}$ by $u_{\rm LO}(\mathbf{s},t) = e^{i\phi}(c/2\pi\hbar\bar{\omega}\bar{n}_{\rm LO})^{1/2}E_{\rm LO}^{(-)}(\mathbf{s},t)$ where $\bar{\omega}$ is the mean signal frequency, assumed much larger than the signal-field bandwidth. The integral in (5), over time and detector surface area A, projects the signal field onto the "spatial-temporal mode" of the local oscillator, $u_{\rm LO}(\mathbf{s},t)$, which is normalized over A and $[0,T]$. The operator $\hat{a}$ defined in this way corresponds to the detected mode. It satisfies the commutation relation for an annihilation operator, $[\hat{a},\hat{a}^\dagger] = 1$.

We have measured $P_\phi(x_\phi)$ for a squeezed signal field and for a vacuum signal field. The squeezed field is generated by using a walk-off compensated, traveling-wave optical parametric amplifier (OPA) consisting of two type-II phase-matched KTiOPO$_4$ (KTP) crystals [13]. The OPA is pumped by 300-ps, near-transform-limited pulses at 532 nm from a frequency-doubled Nd-doped yttrium-aluminum-garnet laser, operating at 420 pulses per second, with energy stability $\pm 3\%$. The generated down-conversion signal centered at 1064 nm consists of two orthogonally polarized fields, the signal and idler, and has a bandwidth estimated to be 10^4 times that of the laser field. The pump polarization and the crystals are oriented such that the produced signal and idler fields are polarized 45° with respect to the polarizer axis (PBS 1). The squeezed field is extracted from the down-conversion field by PBS 1, which also serves to spatially overlap the LO and squeezed field [14]. The LO field (1064 nm, 400 ps) is obtained from the laser beam before frequency doubling, and each LO pulse typically contains a mean number of photons $\bar{n}_{\rm LO} \approx 4 \times 10^6$. The coherent-state shot-noise level (SNL) (variance of photoelectron counts) in our detection scheme is equal to $\bar{n}_{\rm LO}$.

Figure 2 shows our setup for balanced homodyne detection. Precise balancing of total photoelectron numbers from the two detectors (quantum efficiency $\eta \sim 85\%$)
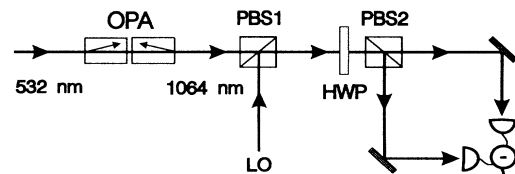

FIG. 2. Apparatus for balanced homodyne measurement of quadrature amplitude. The crystals are oriented at 45° with respect to the polarizer (PBS 1) axes in order to produce the squeezed field. Prisms (not shown) in front of each detector remove the 532 nm pump beam from the 1064 nm signal beam.

is achieved by combining the signal and LO fields with perpendicular polarizations and using a $\lambda/2$ wave plate to rotate these polarizations by 45° [14]. A polarizing beam splitter (PBS 2) interferes the incident fields to produce two fields that are detected by the photodiodes. The photodiode outputs are electronically subtracted and integrated using a low-noise charge-sensitive preamplifier [9], which yields the difference number of photoelectrons on each pulse. Balancing removes most of the additive noise associated with the LO energy fluctuations. Typically the electronic noise variance is 8 times lower than the SNL. We make 4000 repeated measurements of the photoelectron difference number N_ϕ at 27 values of relative phase ϕ, adjusted by moving a mirror on a piezoelectric translator. Using $x_\phi = N_\phi/(2\bar{n}_{\rm LO})^{1/2}$ we thereby obtain estimates of the probability distribution $P_\phi(x_\phi)$. The scaling factor $(\bar{n}_{\rm LO})^{1/2}$ can be measured in two ways: by direct photodiode measurement of $\bar{n}_{\rm LO}$, and by measuring the standard deviation of the photoelectron difference number resulting from the LO field. Our previous experiment showed that these methods agree within 4%. Here we have adopted the latter method, utilizing 160 000 measurements of photoelectron difference number.

Figure 3(a) shows a set of measured distributions of x_ϕ for that mode of the detected squeezed field correspond-

ing to the LO spatial-temporal mode. The variances Δx_ϕ^2 of each distribution are plotted in Fig. 3(b). We also measured $P_\phi(x_\phi)$ for the vacuum input field simply by blocking the down-conversion field and repeating the above procedure. The variances of the vacuum distributions are within 5% of the theoretical value $\Delta x_{\rm vac}^2 = \frac{1}{2}$. For a certain LO phase the variance for the squeezed field is seen to fall 25% below $\Delta x_{\rm vac}^2$ (the SNL). The uncertainty product is $\Delta x_0 \Delta x_{\pi/2} = 0.55$, which is within 10% of the value for a minimum-uncertainty state.

We obtained the Wigner distribution shown in Fig. 1(a) by performing the inverse Radon transform on the measured distributions in Fig. 3(a). The numerical inversion used the standard filtered back projection algorithm for parallel-beam sampling geometry [7]. If $W(x,p)$ is approximately Gaussian, as is expected from theory [15] and verified by our experiment, the analysis in Ref. [16] implies that the 27 values of ϕ and the 64 bins for each $P_\phi(x_\phi)$ are more than sufficient for an accurate reconstruction of $W(x,p)$. The contour plots of $W(x,p)$ clearly show the circular symmetry of the vacuum distribution (within experimental error) and the ellipticity of the squeezed-field distribution. The Wigner distributions are approximately Gaussian, as expected from Eq. (1) with a Gaussian density matrix [15].

A one-dimensional Fourier transform can be performed on $W(x,p)$ to obtain the density matrix for the detected mode,

$$\langle x + x'|\hat{\rho}|x - x'\rangle = \int_{-\infty}^{\infty} W(x,p)e^{2ipx'}dp. \tag{6}$$

Figure 4 shows the magnitude of the resulting density matrices for the vacuum and squeezed states in both x
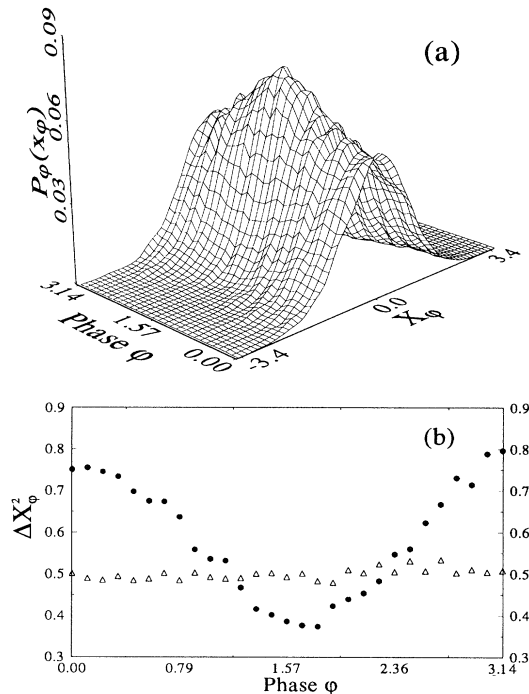

FIG. 3. (a) Measured quadrature-amplitude distributions at various values of local oscillator phase. Note that since these distributions are normalized, a decreasing width of a particular distribution is accompanied by an increase in its peak height. (b) Variances of quadrature amplitude vs LO phase: circles, squeezed state; triangles, vacuum state.
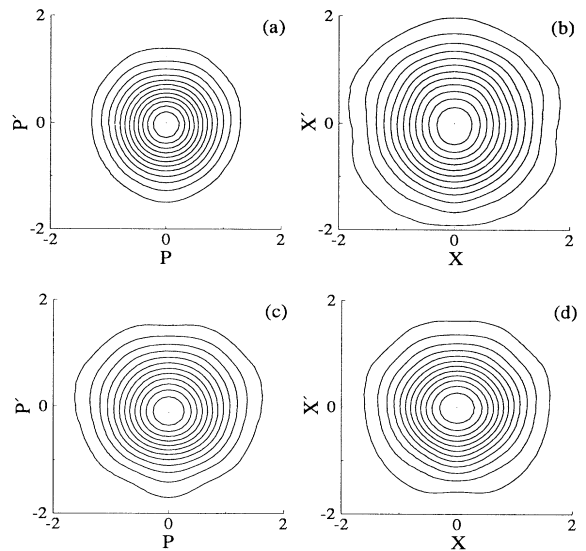

FIG. 4. Measured density matrix for (a),(b) the squeezed state and (c),(d) the vacuum state in x or p representations: (a),(c) $|\langle p + p'|\hat{\rho}|p - p'\rangle|$; (b),(d) $|\langle x + x'|\hat{\rho}|x - x'\rangle|$.

(i.e., $x_\phi=0$) and p ($x_\phi=\pi/2$) representations. They are found to have near circular symmetry in x,x' (or p,p') and to have complex phase angle of less than 0.15π. The vacuum density matrix has the same width in both x and p representations. In the p representation the width of the squeezed-state density matrix is 12% narrower than the width of the vacuum density matrix, while in the x representation it is 18% broader.

Only in the case of a pure state is the density matrix factorizable in the form $\langle x|\hat\rho|x'\rangle=\psi(x)\psi^*(x')$, where $\psi(x)$ is identified as the wave function. Our measured density matrices for the squeezed state are found to be nearly factorizable in this sense. It is not necessarily useful to represent the data in this way since accuracy is lost if this approximate "wave function" is used to make predictions about the field. For the vacuum, which is a pure state, the density matrix is factorizable and we have constructed the wave function in this case. This shows that the wave function for a pure state can in principle be measured.

In conclusion, we have demonstrated that optical homodyne tomography can be used to measure the Wigner distribution, and thereby the density matrix, of a field mode that is selected by the spatial-temporal mode of the local oscillator field. We used OHT to characterize quadrature-squeezed and vacuum states. Given the measured density matrix, one could obtain experimentally *any* of the various quantum distributions of optical phase [11,17]. The method of OHT can also be used for characterizing other quantum states of light such as amplitude-squeezed states, phase-squeezed states, and macroscopic superposition states. The method applies for arbitrary states, including those which have Wigner distributions with negative values. We emphasize that it is the ability to measure quadrature distributions in many different representations which makes this method possible.

[1] For reviews of quadrature- and amplitude-squeezed states see H. J. Kimble, in *Fundamental Systems in Quantum Optics*, edited by J. Dalibard, J. M. Raimond, and J. Zinn-Justin (Elsevier, Amsterdam, 1991); Y. Yamamoto *et al.*, in *Progress in Optics*, edited by E. Wolf (Elsevier, Amsterdam, 1990).

[2] R. Movshovich *et al.*, Phys. Rev. Lett. **65**, 1419 (1990).

[3] K. Vogel and H. Risken, Phys. Rev. A **40**, 2847 (1989).

[4] E. P. Wigner, Phys. Rev. **40**, 749 (1932); M. Hillery, R. F. O'Connell, M. O. Scully, and E. P. Wigner, Phys. Rep. **106**, 121 (1984).

[5] Antoine Royer, Found. Phys. **19**, 3 (1989).

[6] William Band and James L. Park, Found. Phys. **1**, 133 (1970).

[7] F. Natterer, *The Mathematics of Computerized Tomography* (Wiley, New York, 1986).

[8] H. P. Yuen and V. W. S. Chan, Opt. Lett. **8**, 177 (1983).

[9] D. T. Smithey, M. Beck, M. Belsley, and M. G. Raymer, Phys. Rev. Lett. **69**, 2650 (1992).

[10] H. P. Yuen and J. H. Shapiro, IEEE Trans. Inform. Theory, **26**, 78 (1980).

[11] W. Vogel and W. Schleich, Phys. Rev. A **44**, 7642 (1991).

[12] B. Yurke, P. Grangier, R. E. Slusher, and M. J. Potasek, Phys. Rev. A **35**, 3586 (1987).

[13] R. E. Slusher, P. Grangier, A. LaPorta, B. Yurke, and M. J. Potasek, Phys. Rev. Lett. **59**, 2566 (1987); R. E. Slusher, A. LaPorta, P. Grangier, and B. Yurke, in *Squeezed and Nonclassical Light*, edited by P. Tombesi and E. R. Pike, NATO ASI Ser. B, Vol. 190 (Plenum, New York, 1989), pp. 39–53.

[14] P. Grangier, R. E. Slusher, B. Yurke, and A. LaPorta, Phys. Rev. Lett. **59**, 2153 (1987).

[15] First pointed out by R. F. O'Connell, Found. Phys. **13**, 83 (1983).

[16] A Faridani, in *Inverse Problems and Imaging*, Pitman Research Notes in Mathematics Vol. 245, edited by G. F. Roach (Wiley, Essex, 1991), p. 68.

[17] L. Susskind and J. Glogower, Physics (Long Island City, N.Y.) **1**, 49 (1964); D. T. Pegg and S. M. Barnett, Phys. Rev. A **39**, 1665 (1989); W. Schleich, R. J. Horowicz, and S. Varro, Phys. Rev. A **40**, 7405 (1989); J. W. Noh, A. Fougeres, and L. Mandel, Phys. Rev. A **45**, 424 (1992).